Fast Flotation with an Air-sparged Hydrocyclone

by

J.D. Miller and D.J. Kinneberg
University of Utah
U.S.A.

Synopsis

The status of the research programme on air-sparged hydrocyclones at the University of Utah is presented. Fast flotation of coal, oil shale, and copper porphyry ore has been demonstrated with capacities far exceeding those of conventional flotation cells. In addition to the performance characteristics of the air-sparged hydrocyclone, fluid-flow phenomena are reviewed and cost-analysis data are summarized.

INTRODUCTION

Froth flotation is of vital, Worldwide importance for the processing of mineral resources, and now in the United States the installed flotation-plant capacity approaches 2 000 000 t/d divided almost equally between sulphide and non-sulphide flotation plants. Table 1 presents the U.S. flotation-plant capacity for many commodities during the past decades, and it is interesting to note that the major commodities, from a tonnage standpoint, represent each of the well-known flotation systems: sulphides, oxides, salts, and fossil-fuel minerals. The significant increase in non-sulphide flotation-plant capacity during the past two decades is evident. In general, this growth has been observed Worldwide.

TABLE 1

Flotation-plant capacity in the United States

Mineral commodity	Capacity, t/d		
	1960	1970	1980
Copper	168 200	270 000	215 500
Copper–molybdenum	297 500	265 000	622 000
Zinc	28 400	27 100	27 200
Lead–zinc	50 700	35 500	28 700
Iron ore	5 700	55 700	143 700
Phosphate	88 700	305 900	433 900
Potash	39 800	52 200	47 000
Glass sand	3 200	200 200	53 000
Feldspar	5 600	10 000	11 500
Coal	26 500	62 400	78 300
Other	15 040	82 900	142 000
Total	729 340	1 366 900	1 802 800

Since the beginning of flotation technology early in this century, separations have generally been accomplished in aerated stirred-tank reactors—conventional flotation cells. During the past decades, major design changes in the conventional flotation cell were with respect to aeration, agitation, and vessel size or shape[1-3]. R & D efforts have been directed towards scale-up, and now conventional flotation cells of 1500 ft^3 have been installed in some plants.

Other designs of flotation cell without agitators are known[1,4,5], such as the column flotation system, but few are currently installed. Designs to accommodate the difference in bubble-attachment and froth-separation functions have been described, but little attention has been given to the design of fast flotation systems, and, in this regard, the concept of an air-sparged hydrocyclone was presented in 1981[6]. Since that time, experimental evidence suggests that fast flotation in an air-sparged hydrocyclone is possible even with nominal retention times of less than a second.

When conventional flotation in a stirred-tank reactor is considered as a rate process, several important features are evident. Random motion between particles and bubbles results in a low probability for collision and attachment, especially for small particles with low inertia. Bubble-size limitations control the rate of flotation inasmuch as the flotation rate is frequently found to have a significant inverse relation with bubble size. Finally, considerations of air flowrate and dispersion may limit the rate of flotation in conventional flotation cells.

In the air-sparged hydrocyclone, these limitations have been extended to allow for fast flotation owing to directed particle and bubble motion in a centrifugal field, small bubble size, and high flowrate of air. The flotation rate approaches that which would

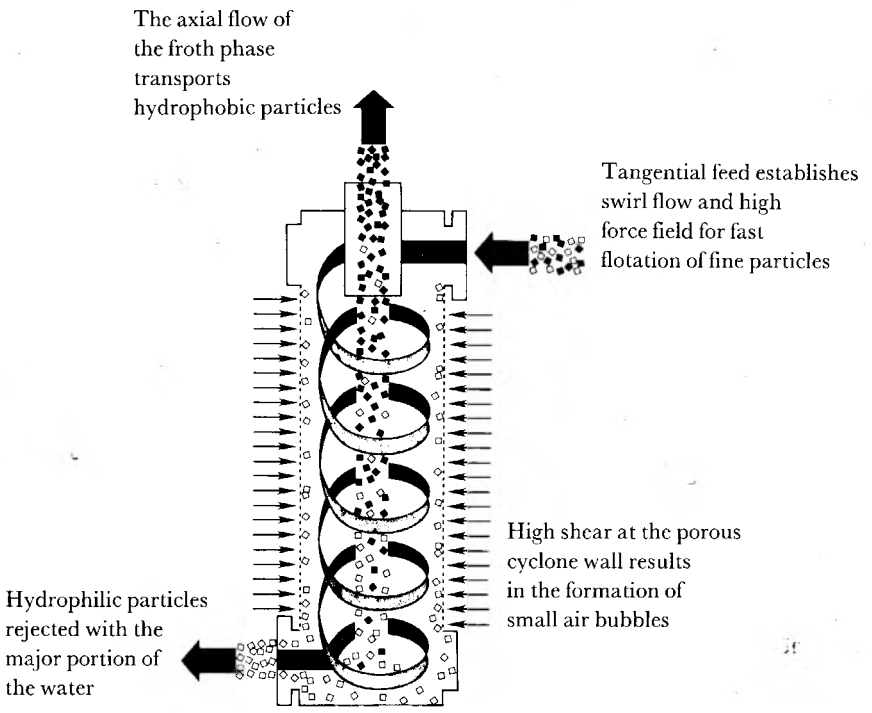

Figure 1. Diagram of the air-sparged hydrocyclone

be limited by bubble-attachment phenomena rather than by collision rate or air flowrate. In essence, flotation separations can be achieved for retention times of the order of seconds rather than minutes. The capacity of the air-sparged hydrocyclone could be 50 to 100 $t/d \cdot ft^3$ compared with 1 to 2 $t/d \cdot ft^3$ for conventional flotation cells.

DESCRIPTION OF THE AIR-SPARGED HYDROCYCLONE

The basic features of the air-sparged hydrocyclone, shown in Figure 1, are a porous wall through which air is sparged and a tangential flow of slurry orthogonal to the air flow. A number of different designs incorporating these features have been tested, and the preferred design is found to be a vertically oriented cylindrical cyclone with the slurry entering the top tangentially.

The slurry, fed tangentially through a conventional cyclone header, passes through the device as a thin layer in a swirl flow. It travels downwards countercurrent to the froth phase, which moves upwards in the centre of the device. Hydrophilic particles are thrown to the porous cylinder wall and are discharged as tailings in the underflow. Hydrophobic particles encounter air bubbles, which are sparged radially through the porous wall. The high shear force at the wall generates small air bubbles and provides for intense interaction between particles and bubbles. Attachment occurs between hydrophobic particles and air bubbles, and the hydrophobic particles are transported into the froth phase, which exists axially at the top of the cyclone through a vortex finder.

The thickness of the swirling layer increases as the multiphase fluid travels down the cylinder. If the constraints at the bottom of the cylinder are removed, this swirling layer can be easily observed. Increasing the rate at which slurry is fed to the cyclone has little effect on the thickness of the swirling layer. However, increasing the rate of air injection increases this thickness dramatically, and, at a sufficiently high rate of air injection, the entire diameter near the bottom of the cylinder is filled with swirling fluid.

Within the layer of swirling fluid, a mass gradient presumably exists because of the centrifugal force field. The region closest to the porous wall contains mostly water, whereas the region near the centre contains mostly air bubbles. Solid particles are distributed within the swirling layer according to their density, size, shape, and interaction with air. Large hydrophilic particles are forced to the wall, while small hydrophilic particles are distributed with the water. Hydrophobic particles must be considered in terms of the mass of the particle-bubble aggregates.

The presumption of a mass gradient gave rise to the annular discharge shown in Figure 2. The point at which the pedestal intersects the gradient is determined by the pedestal's diameter. Increasing the diameter forces more material into the overflow, thereby improving the recovery but lowering the grade of the concentrate. Conversely, decreasing the pedestal diameter allows more material to exit in the underflow.

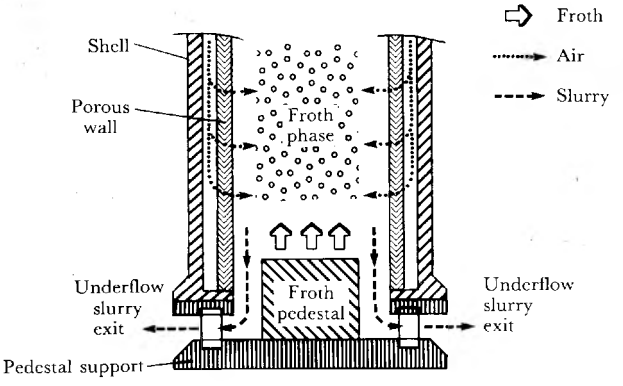

Figure 2. Concept of the annular discharge

FLUID-FLOW BEHAVIOUR

Studies are in progress to describe fluid-flow phenomena related to the performance of the air-sparged hydrocyclone. These studies include both fundamental details and practical aspects of fluid-flow behaviour.

Swirl flow

The basic fluid-flow feature of the air-sparged hydrocyclone is the swirl flow of the system. In the simplest case, a swirl flow of water in a right vertical cylinder results in the formation of a swirling layer, the average thickness of which has been found to be relatively independent of the flowrate and cylinder length for the high centrifugal forces that are of interest[7]. Measurements indicate that the average thickness of this layer is from 2 to 3 mm for a cylinder of 5 cm diameter at flowrates between 50 and 120 l/min and cylinder lengths up to 30 cm. These experimental results are presented in Table 2.

TABLE 2

Measured swirl-layer thickness, in mm, for 5 cm cylinder*

Q_w *(l/min)* $= 24,4\Delta p$ *(lbf/in²)*$^{\frac{1}{2}}$

Axial position distance from inlet cm	Inlet pressure, lbf/in²			
	5	10	15	25
13,7	2,0	2,6	2,5	2,3
18,7	2,1	3,0	3,0	3,1
26,4	1,9	3,0	3,0	2,2

* Accuracy estimated at ± 0,5 mm

Furthermore, it appears that the ratio of tangential to axial velocity does not change with the flowrate.

These experimental results can be predicted from the simple inviscid theory for swirl nozzles proposed by Taylor[8]. From the equations of continuity and conservation of energy and angular momentum, and assuming minimum energy dissipation, Taylor derived the following four equations:

$$Q = \pi(R^2 - r^2)V_a, \quad \ldots\ldots (1)$$

$$\frac{P}{\rho_L} + \frac{V_t^2}{2g} + \frac{V_a^2}{2g} = H_p, \quad \ldots\ldots (2)$$

$$V_t R = \Omega, \quad \ldots\ldots (3)$$

$$\frac{dQ}{dr} = 0, \quad \ldots\ldots (4)$$

where Q is the volumetric flowrate, R and r the radii of the cylinder and the air core, respectively, V_a and V_t the average axial and tangential velocities, P the inlet pressure, H_p the total pressure head, ρ_L the density of the liquid, g the gravitational constant, and Ω a constant. By defining a discharge coefficient, K, by

$$Q = K\pi R^2(2\Delta P/\rho_L)^{\frac{1}{2}}$$

and the dimensionless variables

$$x = \frac{V_a}{U_p}, \; y = \frac{\Omega}{RU_p}, \; z = \frac{r}{R},$$

where $U_p = (2\Delta P/\rho_L)^{\frac{1}{2}}$, Taylor's equations reduce to the following[9]:

$$K = x(1 - z^2), \quad \ldots\ldots (5)$$

$$1 = x^2 + \frac{y^2}{z^2}, \quad \ldots\ldots (6)$$

$$z^2 = \frac{y^2}{4} + \left(\frac{y^4}{16} + \frac{y^2}{2}\right)^{\frac{1}{2}}. \quad \ldots\ldots (7)$$

For a given value of K, these three equations can be solved simultaneously for x, y, and z. Alternatively, one can define a geometric nozzle parameter N as

$$N = \left(\frac{R_1}{R}\right)^2,$$

where R_1 is the radius of the inlet to the cyclone. Then

$$K = Ny. \quad \ldots\ldots (8)$$

For the case of the cylinder under investigation, $N \simeq 0{,}07$. Solving equations (5), (6), and (7) gives

$x = 0{,}32$
$y = 0{,}85$
$z = 0{,}90.$

The predicted swirl-film thickness is therefore $0{,}1\,R$, or 2,5 mm for the cylinder of 5 cm diameter. This compares favourably with the experimentally measured thicknesses shown in Table 2. Also the predicted discharge coefficient (from Equation (8)) of 0,060 compares well with the experimental value of 0,054. More important, though, is the fact that the swirl-layer thickness and the ratio of axial to tangential velocities seems to be independent of the volumetric flowrate.

On the other hand, Taylor's theory does not give any information on the rate of decay of tangential velocity, nor does it accurately predict the actual ratio of tangential to axial velocity. A more detailed

analysis is in progress to provide such additional information.

Bubble formation

Preliminary experiments on bubble formation from single capillaries at the wall of a 5 cm, 20° Plexiglass hydrocyclone have been conducted with a high-speed motor-analyser video system (Spin Physics of Eastman Kodak) having a recording capability of up to 2000 frames per second in full-frame mode and up to 12 000 frames per second in split-frame mode[10]. The parameters studied include the capillary size (340 and 630 μm), solution properties (density, viscosity, surface tension), and flowrate of air (0,1 to 1,2 ml/s). The tangential velocity of the fluid at the point of bubble formation has been measured with laser doppler velocimetry.

A simple theoretical expression for the size of the bubble formed has been derived. It is assumed that, at the high velocities of the continuous phase in the hydrocyclone, the detachment of a bubble from the capillary occurs when the centre of the bubble formed is displaced on its rotational path by a distance equal to the length of the arc with a chord equalling the sum of the radii of the bubble and the capillary. If the effect of surface tension is neglected, an assumption that seems to be verified from the experimental results, the bubble size is given by

$$r_b = \left[\frac{3Q_a}{2V_t} \cdot \sin^{-1}\left\{\frac{r_o + r_b}{2(R_c - r_b)}\right\} \cdot (R_c - r_b)\right]^{\frac{1}{3}}, \quad \ldots\ldots (9)$$

where Q_a = volumetric flowrate of air,
R_c = hydrocyclone radius,
r_b = bubble radius,
r_o = capillary radius,
V_t = tangential velocity of the fluid at the point of bubble formation.

In the case of $R_c > r_b \simeq r_o$, Equation (1) reduces to

$$r_b = \left[\frac{3Q_a(r_o + r_b)}{4V_t}\right]^{\frac{1}{3}}. \quad \ldots\ldots (10)$$

The solution of the cubic equation is

$$r_b = r_o\,(v^*)^{\frac{1}{2}} \cos\left[\frac{\cos^{-1}(9/v^*)^{\frac{1}{2}} + 2\pi k}{3}\right], \; k = 0,\ 1,\ 2, \quad (11a)$$

for $(9/v^*)^{\frac{1}{2}} < 1$,

or

$$r_b = r_o(v^*)^{\frac{1}{2}} \cosh\left[\frac{\cosh^{-1}(9/v^*)^{\frac{1}{2}}}{3}\right], \quad \ldots\ldots (11b),$$

for $(9/v^*)^{\frac{1}{2}} > 1$.

Equation (11) indicates that, for fixed dimensionless velocity v^* (ratio of the air velocity to the tangential water velocity), the bubble size will be proportional to the capillary size.

Typically, for water at a tangential velocity of 2,8 m/s and for an air rate of 1,5 ml/s, the observed and the predicted values of the bubble diameter for a 340 μm capillary are 680 and 686 μm, respectively[10]. This excellent agreement justifies the assumption of a negligible surface-tension effect in the case of gas injection through small-diameter capillaries at these flowrates.

Practical aspects

In some respects, the air-sparged hydrocyclone behaves similarly to the conventional hydrocyclone. As expected, the capacity is related to the pressure drop to the one-half power[7]. Furthermore, water transport to the overflow, though much lower than in a conventional hydrocyclone, appears to have the same linear relation to the feed-water flowrate:

$$Q_w^{OF} = a + bQ_w^F, \quad \ldots\ldots (12)$$

where, for the given cyclone dimensions, a and b are dependent on the addition of frother and the air flowrate. The dependence on the particle size and pulp density has not been established completely. Of course, fine hydrophilic particles will distribute according to the water split, and, in this regard, water to the overflow has a significant impact on the grade of concentrate.

Unlike water transport to the overflow, air to the overflow seems to be independent of the feed-water flowrate (50 to 100 l/min) as well as frother addition (20 to 80 p.p.m.)[7]. In most cases, 85 per cent of the air is recovered in the overflow product, the water content of which can vary from 20 to 50 per cent by volume at ambient pressure. The dependence of air split on the total air flowrate has not been established.

FLOTATION PERFORMANCE

The flotation performance of the air-sparged hydrocyclone has been examined for coal, oil shale, and copper porphyry ore. The most extensive study has been on the copper ore, the results of which are summarized in this section of the paper after consideration of fine-coal cleaning and oil-shale flotation in the air-sparged hydrocyclone.

Coal

The performance of the air-sparged hydrocyclone is compared with the performance of both water-only cyclones and conventional flotation cells in Table 3[11]. Although the extent of ash removal varies with the yield and from coal to coal, it can be noted that much better ash rejection from the finer size intervals is realized with the air-sparged hydrocyclone. Generally, it is reported that water-only cyclones are ineffective for ash and sulphur rejection from coals finer than 100 mesh.

TABLE 3

Comparison of coal-cleaning efficiency of the air-sparged hydrocyclone (A.S.H.) with conventional coal technologies

Particle size mesh	Ash removal				
			15 cm A.S.H.		
	Water-only cyclone %	Single-stage flotation %	Illinois no. 6 %	Beaver Creek %	Lower Kittaning %
28–100	60–65	50–60	77–86	84	71
100–200	40–45	40–45	59–68	70	40
200–325	15–18	40–45	44–62	77	43
<325	0–5	50–55	57–67	81	54

Typical performance of the air-sparged hydrocyclone with respect to the particle size is shown in Figure 3. It is noted that the recovery is reduced at coarser particle sizes. Nevertheless, good ash removal is realized at all particle sizes except the fraction smaller than 400 mesh. Contamination of the clean coal with ash from that fraction results from the transport of fine hydrophilic particles by water into the froth phase.

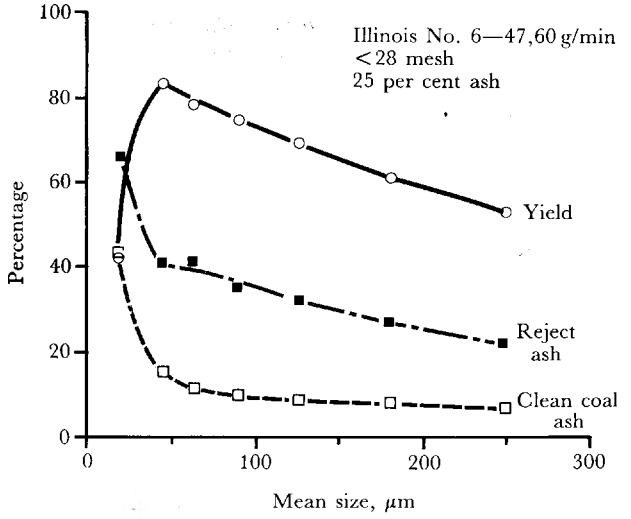

Figure 3. Yield, clean-coal ash content, and reject ash content as functions of the particle size for the 15 cm air-sparged hydrocyclone

Also, good rejection of pyritic sulphur from a high-sulphur Midwestern coal has been realized. Air-sparged hydrocyclone flotation of the coal smaller than 28 mesh, which has a pyritic sulphur content of about 3,0 per cent, was equivalent to the flotation results obtained with bench-scale flotation in a conventional cell in which a 65 per cent rejection of pyritic sulphur was achieved.

Oil shale

A preliminary study of oil-shale concentration by flotation in an air-sparged hydrocyclone has been reported[12]. Oil shale is an intimate mixture of organic material—kerogen—with inorganic shale minerals and is being considered as a possible energy resource. Grinding to 10 micrometres is frequently required to achieve a satisfactory level of liberation. The flotation separation efficiency of such fine particles with an air-sparged hydrocyclone has been shown to be equivalent to that obtained with a conventional flotation cell.

Copper porphyry ore

The most extensive study of the air-sparged hydrocyclone has been the flotation response of a low-grade copper porphyry (Cu at 0,7 per cent) with a 5 cm air-sparged hydrocyclone as a function of both the operating and design variables[13]. The ore was typical flotation-plant feed, 80 per cent passing 65 mesh. A typical flotation reagent schedule was selected, with the exception that a higher frother level and addition of fuel oil improved both the recovery and the concentrate grade.

The influence of the slurry feed rate on the recovery of copper as a function of the particle size is presented in Figure 4. As indicated, recoveries higher than 80 per cent can be obtained for particles less than 100 micrometres in diameter, approaching 100 per cent for particles in the interval 150 to 400 mesh. The recoveries drop off quickly

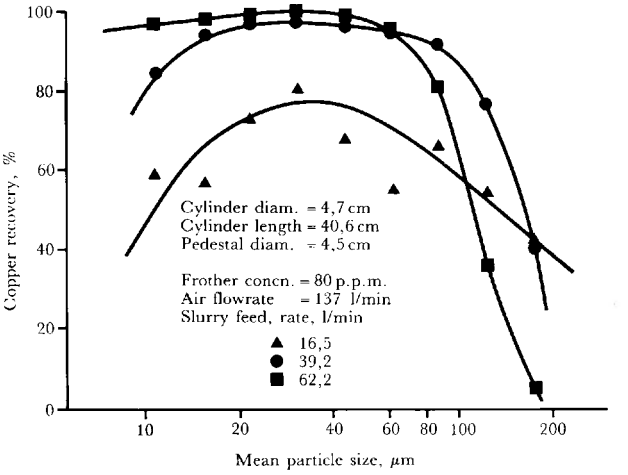

Figure 4. Effect of the slurry feed rate on the copper recovery as a function of the particle size

for particles larger than 100 micrometres and rather slowly for particles smaller than 400 mesh. As the slurry feed rate is increased, so increasing the centrifugal force within the cyclone, the recovery curve shifts to the left, the recoveries being lower for large particles and higher for fine particles. The copper recovery for particles larger than 400 mesh increases with an increase in cyclone length up to an L/D ratio of 15:1, but the recovery of copper for particles smaller than 400 mesh appears to be independent of the cyclone length.

The experimental data indicate that increasing the centrifugal force effectively breaks down the interaction between large particles and bubbles. Particles are stripped off the bubble surface, and the recovery is reduced, regardless of the air flowrate. Conversely, an increased centrifugal field enhances the recovery of fine particles. This can be explained in terms of a decrease in the bubble size with an increased flowrate and an increase in inertia for the particles, leading to an increased collision efficiency. The increase in recovery for fine particles shown in Figure 4 is not due to an increased water split, since the fraction of water reporting to the overflow actually decreased with increasing slurry feed rate.

An interpretation of these results can also be based on the work of Schubert[14] concerning the influence of turbulence in flotation. According to Schubert's observations, the flotation of large particles requires low levels of turbulence. Hence it would be expected that the recovery of large particles would be diminished as the slurry feed rate (and thereby the level of turbulence) is increased. On the other hand, Schubert indicates that the flotation of fine particles requires a high degree of turbulence to maximize collisions between particles and bubbles. Here again the experimental results follow the expected pattern.

The effect of increased slurry feed rate on the overall copper grade is presented in Figure 5. The grade of all particle-size intervals, except the coarse sizes, is enhanced with increased centrifugal force. This can be regarded as a centrifugal cleaning action. Hydrophilic particles, physically entrained in the froth phase, are stripped away by the centrifugal force and thrown against the porous wall to report to the underflow. The optimal centrifugal force (or slurry feed rate) is one that balances the rupture of attachments between hydrophobic particles and bubbles with the cleaning action on misplaced hydrophilic particles. Interestingly, it is the size fractions that are the most easily recovered which display the highest grades.

Experiments were performed to determine the effect of pulp density with cell lengths of 68 and 97 cm. The pulp density ranged from 5 to 30 on the basis of mass percentage of solids. The slurry feed rates ranged from 48 to 67 kg/min while the air flowrate was held constant at about 200 l/min. A pedestal diameter of 4,32 cm was used. The results are presented in Figure 6. As indicated, the copper recovery did not decrease with increasing pulp density. On the contrary, the recovery of particles both larger and smaller than 400 mesh showed an increase with increasing solid content, other variables being held constant. However, the overall copper grade of the concentrate decreased from between 6 and 8 per cent at 5 per cent solids to between 2 and 3 per cent at 30 per cent solids.

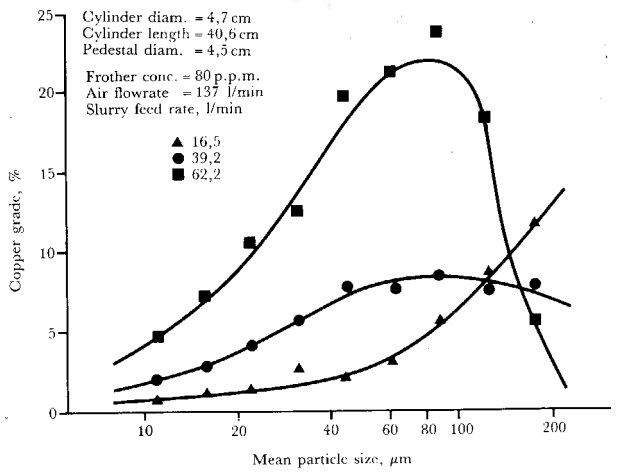

Figure 5. Concentrate grade as a function of particle size for various slurry feed rates

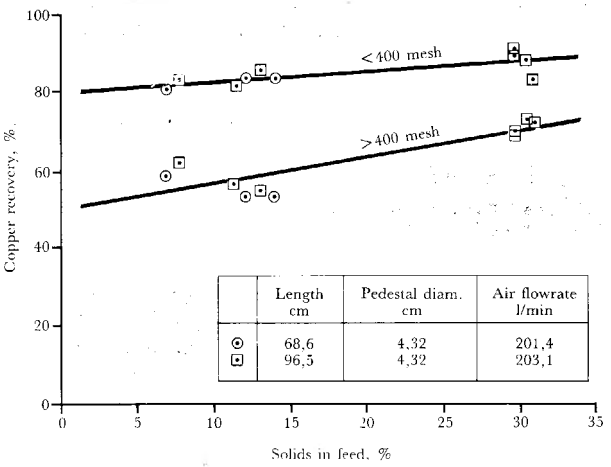

Figure 6. Influence of solids in the feed on the copper recovery for coarse and fine particles

These results indicate that reasonably high pulp densities (20 to 30 per cent by mass of solids) should not limit the performance of the air-sparged hydrycyclone. A high solid content appears to increase the thickness of the swirl layer against the porous wall and thereby, at a fixed pedestal size, force more material into the overflow stream. This would explain the drop in the concentrate grade. In addition, the results could be interpreted in terms of a turbulence damping effect associated with increased amounts of small particles. Thus the recovery of large particles would be expected to increase. The increase in the recovery of fine particles could be attributed to an increased water split.

Copper porphyry ores frequently carry molybdenum and gold values, which are recovered as

TABLE 4

Comparison of flotation response for copper and molybdenum by particle size

Slurry feed rate = 51,6 l/min
Air flowrate = 178 l/min
Frother concentration = 80 p.p.m.
Pedestal diameter = 4,5 cm
Cylinder diameter = 4,7 cm
Cylinder length = 40,6 cm

Particle size interval mesh	Copper			Molybdenum		
	Grade, %		Recovery %	Grade, %		Recovery %
	OF	UF		OF	UF	
>100	19,09	0,303	16,8	2,011	0,0067	49,2
100–200	28,48	0,200	83,4	0,632	0,0010	95,4
200–400	23,40	0,040	97,5	0,409	0,0060	97,8
<400	4,63	0,150	89,8	0,079	0,0043	83,9
Overall	8,04	0,193	82,3	0,163	0,0038	83,7
Head	0,99		100,0	0,020		100,0
Ratio $\frac{\text{feed}}{\text{conct.}}$ = 9,9						

OF = Overflow
UF = Underflow

byproducts. Both of these components are recovered with the air-sparged hydrocyclone at an efficiency comparable with that observed for copper. For example, Table 4 presents a side-by-side comparison of copper and molybdenum recovery as a function of the particle size for a particular annular-discharge experiment. It can be seen that the molybdenum recovery was substantially higher than the copper recovery in the two coarsest size intervals, about the same in the interval between 200 and 400 mesh, and somewhat lower for material smaller than 400 mesh. The overall molybdenum recovery was equal to the overall copper recovery.

The performance of the air-sparged hydrocyclone is compared with the performance of a continuous conventional flotation cell as shown in Figure 7. The recovery as a function of the retention time (log scale) vividly demonstrates the significant difference in flotation rate and accounts for the high capacity of the air-sparged hydrocyclone.

Figure 8 completes the comparison by presenting grade and recovery curves for the air-sparged hydrocyclone and for conventional flotation cells. The air-sparged hydrocyclone gives grades that are comparable with those obtained with conventional flotation. However, it should be noted that industrial operations achieve Cu grades in the range of 15 to 20 per cent at recoveries exceeding 80 per cent for rougher flotation by using several cells in each bank. This arrangement has not yet been tested for air-sparged hydrocyclones.

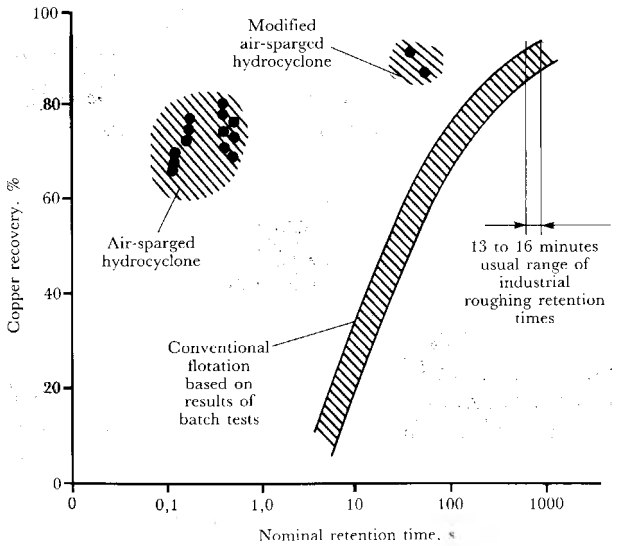

Figure 7. Comparison of recoveries with the air-sparged hydrocyclone as a function of the retention time with those predicted for conventional continuous flotation based on batch tests

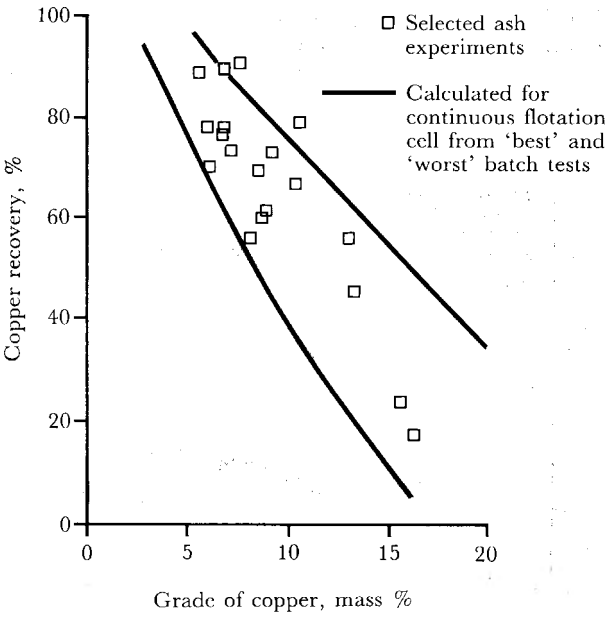

Figure 8. Comparison of grade-recovery curves for conventional continuous cells with experimental data from the air-sparged hydrocyclone

ECONOMIC ANALYSIS FOR FLOTATION OF COPPER PORPHYRY ORE BY AIR-SPARGED HYDROCYCLONE

A preliminary economic analysis is useful in determining whether new processes are feasible and, if so, which variables are economically significant. Besides identifying areas where information is lacking, the analysis can direct research towards reducing the projected costs.

With this in mind, a preliminary economic analysis was performed for the air-sparged hydrocyclone as an alternative to conventional froth flotation[15]. The concentration of a low-grade copper porphyry ore was selected for study because of the abundance of available technical data, for both conventional and air-sparged-hydrocyclone flotation. The variables of interest included the cyclone size, consumption of compressed air, and slurry density (percentage solids).

The calculation of the size of an air-sparged hydrocyclone requires scale-up relations. At present, these relations do not exist; but some educated guesses can be made. Under the assumption that the air-sparged hydrocyclone behaves similarly to a conventional hydrocyclone (evidence supporting this assumption includes the form of the equation connecting pressure drop and capacity, the shape of the classification curves, and the influence of the flowrate on the cut-size), it can be argued that the scale-up equations for a conventional hydrocyclone are applicable to the air-sparged hydrocyclone. Moreover, it seems logical to propose cut-size equivalence as the scale-up criterion, since the cut-size reflects the centrifugal forces present in a cyclone. A review of the literature[15] shows that size-capacity equations for a conventional cyclone have the form

$$Q \propto D^n, \quad \ldots\ldots\ldots\ldots\ldots\ldots\ldots\ldots\ldots\ldots\ldots\ldots \quad (13)$$

where Q is the volumetric flowrate and D the diameter of the cyclone. The exponent n usually ranges from 2,5 to 3,1. As a conservative estimate, n was taken to be 2,5. The next step in scale-up involves estimating the operating pressures. If the cut-size is held constant, the pressure of the cyclone must be increased as the cyclone diameter is increased. It is commonly accepted[16] that

$$\Delta P \propto \frac{Q^2}{D^4}. \quad \ldots\ldots\ldots\ldots\ldots\ldots\ldots\ldots\ldots\ldots\ldots\ldots \quad (14)$$

Substituting Equation (13) into (14) with $n = 2,5$ shows that ΔP is directly proportional to the diameter. This result leads to the expectation that the size of air-sparged cyclones will probably be limited by pressure constraints.

To determine the relative economic advantages of the air-sparged hydrocyclone, the installed cost and energy consumption for four conceivable air-sparged-hydrocyclone circuits were estimated. These costs and energy consumptions were then compared with those of a conventional flotation circuit. A complete economic analysis including a return-on-investment computation was not performed, because of the lack of data on the maintenance costs associated with the porous walls of air-sparged hydrocyclones. Estimates of the installed costs were derived from the costs of purchased equipment taken from vendors and the literature[17,18] multiplied by material and labour factors[19]. These costs do not contain indirect costs, contingencies, or contractors' fees. Also, costs associated with plant buildings were not included.

The material balance and equipment list of the conventional flotation plant were taken from the literature[19], with the following exceptions:

- ten-minute (as opposed to twelve-minute) residence times were assumed for rougher and scavenger circuits,
- 1500-cubic-foot flotation cells were used for rougher and scavenger circuits with 1200-cubic-foot and 1000-cubic-foot cells for cleaners, and
- the power consumption was estimated at 0,06 installed horsepower per cubic foot of cell for the rougher and scavenger cells, and 0,07 for the cleaner cells.

The assumed material balance and circuit configuration corresponding to this conventional flotation alternative are represented schematically in Figure 9. The material balance for the air-sparged-hydrocyclone circuit was based on experimental data obtained in a cyclone of 5 cm diameter operated with

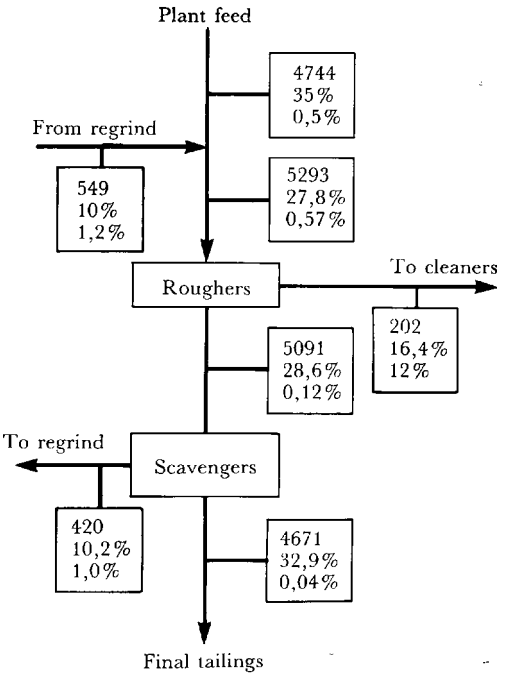

Key: Dry solid, t/h
Mass percent solid, %
Copper grade, %

Figure 9. Assumed material balance and circuit configuration for the conventional flotation base case

an underflow-collection sump[13]. In these experiments, feed slurry at 20 per cent solids was injected at 6 to 8 lbf/in^2. The overflow product contained about 80 per cent of the feed copper at a copper grade of 7 per cent. The underflow discharged into a sump in which these formed a froth product containing an additional 10 per cent of the feed copper. This material, termed a secondary concentrate, corresponds to a scavenger concentrate. The full-scale air-sparged cyclone circuit was designed to follow these tests, as shown in Figure 10.

Three different sets of operating conditions of the air-sparged hydrocyclones were considered. In the first set, the units would be operated at a slurry-feed pressure of 60 lbf/in^2 and an air pressure of 40 lbf/in^2. The normal experimental conditions have been in the range of 10 and 30 lbf/in^2, respectively. The cyclone diameter was specified at 20 inches, requiring air at 1,5 l/min for every l/min of slurry. In the second set, the slurry-feed pressure was reduced to 30 lbf/in^2, at the same air pressure (40 lbf/in^2). Finally, in the third alternative considered, the air pressure was also decreased to 20 lbf/in^2.

Estimates of the capital costs and installed power requirements for the conventional plant and the three air-sparged hydrocyclone alternatives are presented in Table 5 as percentages of the total conventional plant value.

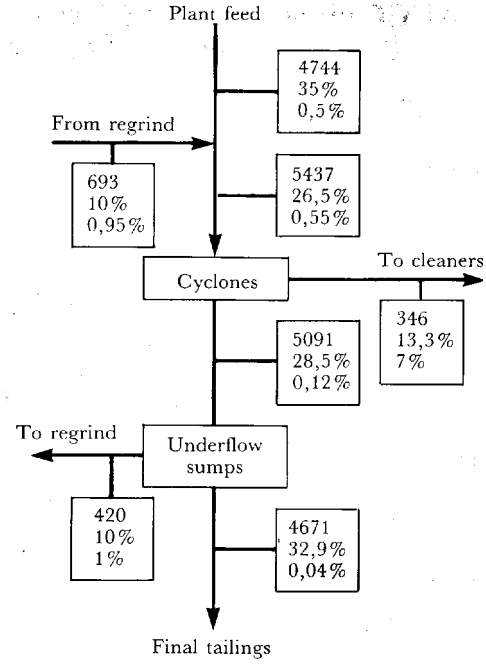

Key: Dry solid, t/h
Mass percent solid, %
Copper grade, %

Figure 10. Assumed material balance and circuit configuration for the air-sparged hydrocyclone alternative

TABLE 5

Summary of preliminary economic analysis (values given as per cent of conventional case)

	Conventional flotation*	Air-sparged hydrocyclones†		
		Case 1	Case 2	Case 3
Capital cost‡				
Roughers	42	19	25	25
Scavengers	40	5	7	7
Cleaners	9	16	16	16
Pumps	9	17	26	26
Compressor	–	8	8	5
Total	100	65	82	79
Installed horsepower§				
Roughers	41	–	–	–
Scavengers	38	5	7	7
Cleaners	8	15	15	15
Pumps	13	66	42	42
Compressor	–	11	11	6
Total	100	97	75	70

* Based on material balance given in: ARBITER, N., *et al.* Conceptual design of flotation circuits. *MINERAL PROCESSING PLANT DESIGN. Mular, A.L., and Bhappu, R.B. (eds.).* New York, AIME, Society of Mining Engineers, 1980. pp. 447–465.

† Based on material balances extrapolated from experimental data (see Figure 10).
Case 1: 60 lbf/in^2 slurry-feed pressure, 40 lbf/in^2 air pressure.
Case 2: 30 lbf/in^2 slurry-feed pressure, 40 lfb/in^2 air pressure.
Case 3: 30 lbf/in^2 slurry-feed pressure, 20 lbf/in^2 air pressure.

‡ Purchased equipment cost times material and labour factor as defined in: GUTHRIE, K.M. Capital cost estimating. *Chem. Eng. (Albany),* vol. 76. Mar. 1969. pp. 114–142.

§ Based on 0,06 hp/ft^3 for rougher and scavenger cells, 0,07 hp/ft^3 for cleaner cells. A.S.H. feed pump power estimated from flow and twice the A.S.H. feed pressure.

As indicated, even under the extreme assumed conditions of Case 1 (60 lbf/in^2 slurry pressure and 40 lbf/in^2 air pressure), a saving of 20 per cent in the capital cost is to be expected when compared with conventional flotation. The air-sparged hydrocyclone being a high-capacity device, these savings result from a lower investment in the rougher and scavenging units. Any savings in floor space were not included in the analysis. In Case 2, a slightly higher capital cost is projected because of the decrease in the processing capacity at lower inlet pressures. In Case 3, additional savings result from the reduced expected consumption of air. In terms of operating cost—examined here on the basis of the expected consumption of energy—the air-sparged hydrocyclone also appears to be quite attractive. For the first case, the cost of the energy is almost equal to the cost in conventional flotation. However, for the more optimistic cases, savings up to 30 per cent are to be expected.

Although the results shown in Table 5 represent a large number of assumptions (believed to be conservative assumptions), it can be concluded that an air-sparged-hydrocyclone circuit could be cost effective. Future research into the optimization and scale-up of air-sparged hydrocyclones is therefore justifiable.

SUMMARY

The fast flotation of fine particles with the air-sparged hydrocyclone has been demonstrated for the concentration of coal, oil shale, and copper porphyry ore. The experimental results indicate that the separation efficiency is comparable with that obtained by conventional flotation. Most significantly, capacities of 50 t/(d·ft^3) could be expected for the air-sparged hydrocyclone compared with 1 t/(d·ft^3) for conventional flotation cells. Economic analysis suggests that air-sparged hydrocyclones are potentially cost effective for the flotation of copper porphyry ore.

Fundamental studies of swirl flow and bubble formation will provide additional insights into the improved design and operation of the air-sparged hydrocyclone. From the inviscid theory for swirl nozzles, the thickness of the swirl layer in a right vertical cylinder, such as is used in the air-sparged hydrocyclone, is expected to be of the order of 0,1 times the cylinder radius. Studies of bubble formation in swirl flow continue to provide information regarding the effect of fluid flow on the relation between bubble size and pore size. Depending on the ratio of the air velocity to the water velocity, the bubble size may be larger than or less than the pore size.

Particle-bubble attachment and transport to the froth phase involve complex phenomena, including:

- centrifugal force field—increased particle and bubble inertia—,
- the generation of numerous small air bubbles by high shear force at the porous wall surface,
- directed rather than random interaction of particles with the freshly formed air bubbles at the porous wall surface, and
- the transport of particle-bubble aggregates a short distance through the layer of slurry in swirl flow into the froth phase.

These contribute to the rapid flotation of fine hydrophobic particles. In the hydrocyclone's centrifugal field, the slurry, in swirl flow, encounters the radial flow of air through the porous cylinder wall. The high shear forces at this surface generate numerous small bubbles and provide for directed particle-bubble interaction. Aggregates of hydrophobic particles and air bubbles are transported through the thin film of slurry into the froth phase, which moves countercurrent to the pulp and exists axially in the overflow. The hydrophilic particles remain in swirl flow and exit in the underflow at the bottom of the air-sparged hydrocyclone.

ACKNOWLEDGEMENTS

This research activity has been supported by funds from the Particulate and Multiphase Processes Program National Science Foundation, Grant No. 82-13963, as well as by funds from the U.S.B.M., Grant No. G1115492. Thanks are extended to K. Upadrashta and S. Gopalakrishnan for the use of their early research findings on bubble formation in swirl flow. Laboratory assistance from J. Allen and D. Wayment and preparation of the manuscript by K. Argyle has been appreciated. The cost analysis was accomplished with the assistance of J.E. Sepulveda.

REFERENCES

1. YOUNG, P. Flotation machines. *Min. Mag. (Lond.)*, vol. 146. Jan. 1982. pp. 35-59.
2. HARRIS, C.C. Flotation machines. *FLOTATION, A.M. GAUDIN MEMORIAL VOLUME. Fuerstenau, M.C. (ed.).* New York, AIME, Society of Mining Engineers, vol. 2. 1976. pp. 753-815.
3. LLOYD, P.J.D., HINDE, A.L., and HEBDEN, D. The design and scale-up of the Chamber of Mines flotation cell. Presented at the *SAIMM SYMPOSIUM ON FLOTATION.* Sep. 1983.
4. IOHN, P. Achievements made in the development of flotation cells without agitator. *Aufbereitungs—Tech.*, vol. 14, no. 3. 1973. pp. 156-161.
5. BAHR, A., LÜDKE, H., and MEHRHOFF, F.W. The development and introduction of a new coal flotation cell. *PROCEEDINGS 14TH INTERNATIONAL MINERAL PROCESSING CONGRESS,* Toronto, Canada, 1982. Montreal, Canadian Institute of Mining and Metallurgy, vol. 5. 1982. Paper no. VII-5. pp. 1-14.
6. MILLER, J.D. The concept of an air-sparged hydrocyclone. Paper presented at the *110TH AIME ANNUAL MEETING,* Chicago. Feb. 1981. pp. 1-10.

7. KINNEBERG, D.J. Froth flotation in an air-sparged hydrocyclone. Ph.D. thesis, University of Utah, 1984. (To be completed.)
8. TAYLOR, G.I. *PROCEEDINGS 7TH INTERNATIONAL CONGRESS ON APPLIED MECHANICS,* London, Imperial College. 1948. p. 280.
9. KOH, P.T.L., and UHLHERR, P.H.T. The discharge coefficient of a gas-liquid swirl nozzle used for gas dispersion. *Chem. Eng. J.,* vol. 14. 1977. pp. 31-40.
10. MILLER, J.D., UPADRASHTA, K.R., and GOPALAKRISHNAN, S. Bubble formation at the wall of an air-sparged hydrocyclone. *PROCEEDINGS PACIFIC REGION MEETING OF THE FINE PARTICLE SOCIETY.* Aug. 1983.
11. MILLER, J.D., and VAN CAMP, M.C. Fine coal flotation in a centrifugal field with an air-sparged hydrocyclone. *Min. Eng.* (N.Y.), vol. 34, no. 11. Nov. 1982. pp. 1575-1580.
12. MISRA, M., LIN, C.L., and MILLER, J.D. Concentration of eastern oil shale by froth flotation, *PROCEEDINGS EASTERN OIL SHALE SYMPOSIUM,* Lexington, Kentucky. Nov. 1983.
13. KINNEBERG, D.J., and MILLER, J.D. Copper sulphide flotation in an air-sparged hydrocyclone. *USBM Final Report on Grant* G1115492. May 1983.
14. SCHUBERT, H. Hydrodynamics of flotation processes. *Aufbereitungs—Tech.* vol. 20, no. 5. 1979. pp. 252-260.
15. KINNEBERG, D.J., and MILLER, J.D. Performance and cost analysis of the air-sparged hydrocyclone for the flotation of low-grade copper porphyry ore. *AIME ANNUAL MEETING,* Los Angeles. Feb. 1984. (To be presented.)
16. BRADLEY, D. The hydrocyclone. Oxford, Pergamon Press. 1965.
17. MULAR, A.L. Mining and mineral processing equipment costs and preliminary capital cost estimations. Special vol. 25. Montreal, Canadian Institute of Mining and Mettallurgy. 1982.
18. RICHARDSON ENGINEERING SERVICES. Process plant construction and estimating standards, vol. 4. 1982.
19. GUTHRIE, K.M. Capital cost estimating. *Chem. Eng.* (Albany), vol. 76, no. 6. Mar. 1969. pp. 114-142.
20. ARBITER, N., HOBSBAWN, P.B., MAHONEY, J.F., and HARRIS, C.C. Conceptual design of flotation circuits. *MINERAL PROCESSING PLANT DESIGN.* 2nd edition. *Mular, A.L., and Bhappu, R.B. (eds.).* New York, AIME, Society of Mining Engineers. 1980. pp. 447-465.